

Effects of Drop-size Distribution and Climate on Millimeter-wave Propagation Through Rain

E. J. Dutton



U.S. DEPARTMENT OF COMMERCE
Malcolm Baldrige, Secretary

Alfred C. Sikes, Assistant Secretary
for Communications and Information

August 1986

TABLE OF CONTENTS

	PAGE
ABSTRACT	1
1. INTRODUCTION AND BACKGROUND	1
2. PARABOLIC DROP-SIZE DISTRIBUTION MODEL	2
3. APPLICATION OF THE PARABOLIC MODEL	4
4. CLIMATIC CHARACTERIZATION OF ATTENUATION DISTRIBUTIONS	11
5. ANALYSIS OF RECENT RAIN ATTENUATION DISTRIBUTIONS	14
5.1 Distributional Analysis at Gasquet, California	14
5.2 Distributional Analysis at Boulder, Colorado	21
6. CONCLUSION	29
7. ACKNOWLEDGMENTS	30
8. REFERENCES	30

LIST OF FIGURES

FIGURE		PAGE
1	Plots of the drop-size density function (lower left-hand plot) obtained from $n(D) = b_1 D^2 + b_2 D + b_3$ and the Marshall and Palmer (1948) model, and of the specific attenuation versus frequency (upper right-hand plot) at Gasquet, CA, February 6, 1985, 2127 hours local time, for a rain rate $R = 7.34$ mm/h.	6
2	Same as Figure 1 at Gasquet, CA, but for March 20, 1985, 1314 hours local time, for a rain rate $R = 2.96$ mm/h.	7
3	Same as Figure 1 at Gasquet, CA, but for March 23, 1985, 1828 hours local time, for a rain rate $R = 33.26$ mm/h.	8
4	Same as Figure 1 at Gasquet, CA, but representing the 0.1% ($R = 27.2$ mm/h) expectancies of specific attenuation and rain rate.	9
5	A three-rainfall zonal division of CONUS for millimeter-wave rain attenuation prediction purposes. Small circles indicate some major urban weather-observing locations in CONUS.	13
6	Quadratic regression best-fit (curve A) and 99.95% prediction bound (curve B) to the January 27 to March 26, 1985, sample of daily specific rain attenuation distributions for Gasquet, CA, at 28.8 GHz.	15
7	Quadratic regression best-fit (curve A) and an empirically derived upper bound distribution (curve B) for the January 27 to March 26, 1985, sample of daily specific rain attenuation distributions for Gasquet, CA, at 28.8 GHz.	16
8	Quadratic regression best-fit (curve A) and 99.95% prediction bound (curve B) to the January 27 to March 26, 1985, sample of daily specific rain attenuation distributions for Gasquet, CA, at 57.6 GHz.	17
9	Quadratic regression best-fit (curve A) and an empirically derived upper bound distribution (curve B) for the January 27 to March 26, 1985, sample of daily specific rain attenuation distributions for Gasquet, CA, at 57.6 GHz.	18
10	Quadratic regression best-fit (curve A) and 99.95% prediction bound (curve B) to the January 27 to March 26, 1985, sample of daily specific rain attenuation distributions for Gasquet, CA, at 96.1 GHz.	19
11	Quadratic regression best-fit (curve A) and empirically derived upper bound distribution (curve B) for the January 27 to March 26, 1985, sample of daily specific rain attenuation distributions for Gasquet, CA, at 96.1 GHz.	20

- 12 Quadratic regression best-fit (curve A) and 99.95% prediction bound (curve B) to the May 19 to July 24, 1985, sample of daily specific rain attenuation distributions for Boulder, CO, at 28.8 GHz. 22
- 13 Quadratic regression best-fit (curve A) and an empirically derived upper bound distribution (curve B) for the May 19 to July 24, 1985, sample of daily specific rain attenuation distributions for Boulder, CO, at 28.8 GHz. 23
- 14 Quadratic regression best-fit (curve A) and 99.95% prediction bound (curve B) to the May 19 to July 24, 1985, sample of daily specific rain attenuation distributions for Boulder, CO, at 57.6 GHz. 24
- 15 Quadratic regression best-fit (curve A) and an empirically derived upper bound distribution (curve B) for the May 19 to July 24, 1985, sample of daily specific rain attenuation distributions for Boulder, CO, at 57.6 GHz. 25
- 16 Quadratic regression best-fit (curve A) and 99.95% prediction bound (curve B) to the May 19 to July 24, 1985, sample of daily specific rain attenuation distributions for Boulder, CO, at 96.1 GHz. 26
- 17 Quadratic regression best-fit (curve A) and an empirically derived upper bound distribution (curve B) for the May 19 to July 24, 1985, sample of daily specific rain attenuation distributions for Boulder, CO, at 96.1 GHz. 27

EFFECTS OF DROP-SIZE DISTRIBUTION AND CLIMATE
ON MILLIMETER-WAVE PROPAGATION THROUGH RAIN

E.J. Dutton*

The distribution of raindrop sizes in a given volume of air remains an unknown aspect of critical importance to the prediction of rain attenuation at millimeter-wave frequencies. Thus, in this report, the search continues for a methodology of predicting drop-size distribution with more apparent success than with earlier procedures developed by this author. The latest method involves prediction of the coefficients of a quadratic fit to the drop-size distribution.

Climatology of rain attenuation also is pursued in this report, with more data from the Institute for Telecommunication Sciences (ITS) millimeter-wave experiment undergoing analysis and statistical examination to try to determine bounds on the specific attenuation that could be expected in a maritime climate (Gasquet, CA) and a dry-continental, temperate climate (Boulder, CO). The data analyzed were all taken in 1985 at the three frequencies of 28.8, 57.6, and 96.1 GHz. Observed data were lumped into 1-min average specific rain attenuations for analysis purposes in this report.

Key Words: attenuation climatology; attenuation distribution;
 millimeter waves; rain attenuation; raindrop size distribution

1. INTRODUCTION AND BACKGROUND

In the past couple of years, methods that involve matrix solution of equations relating the specific attenuation measured at three millimeter-wave frequencies and the theoretical relationship of individual raindrop cross-sections integrated over the distribution of raindrop sizes in a given volume of air have been introduced (Dutton and Steele, 1984). The first of these methods has proven relatively unsuccessful (Dutton, 1986), so that now a second method, as described in Sections 2 and 3 of this report, has been developed with apparently better success. The second method is roughly analogous to the first method, but the fundamental approach is somewhat dissimilar, being designed to represent the entire volumetric raindrop size spectrum rather than just a very few values in it.

One of the major purposes of the millimeter-wave propagation experimentation at the Institute for Telecommunication Sciences (Espeland et al., 1986) has been to develop millimeter-wave propagation characteristics through rain-

*The author is with the Institute for Telecommunication Sciences, National Telecommunications and Information Administration, U.S. Department of Commerce, Boulder, Colorado 80303-3328.

fall across the conterminous United States of America (CONUS). This requires a rainfall attenuation climatology in CONUS. However, this climatology must be achieved within budgetary constraints, yet be of sufficient breadth to represent CONUS. It is believed that this can be minimally achieved by measurement of three rain-climate types as discussed in Section 4. There appears, at the time of this writing, to be sufficient data for the analysis of two of these climatic types. Data from the Huntsville, Alabama, site have as yet been too sparse for the statistical analysis procedure used on the other data discussed in Section 5.

2. PARABOLIC DROP-SIZE DISTRIBUTION MODEL

In Dutton (1986), a quadrature method (Westwater and Strand, 1972) was used to attempt to determine four representative values of the path-averaged raindrop size distribution (or density function) from measurements of rain attenuation at 28.8, 57.6, and 96.1 GHz. Details of the measurement process and results are described in Dutton (1986), Espeland et al., (1986) and in Section 4 of this report, but are not particularly germane to this section of the report.

The method of Dutton and Steele (1984) was reexamined in Dutton (1986) with the conclusion that the data sample was far too small, in the frequency sense, to provide meaningful results across the drop-size spectrum. Perhaps a better approach would be to try to find an analytic representation of the drop-size distribution and determine the coefficients of this representation. If we use a parabolic representation of the form

$$n(D) = b_1 D^2 + b_2 D + b_3, \quad (1)$$

we will have three coefficients, b_i ($i = 1$ to 3), for the three measurement frequencies ν_i to describe the drop-size density function, $n(D)$. The function $n(D)$ is defined as the number of spherical raindrops per cubic meter of air per centimeter of diameter between diameters D and $D + dD$. We shall usually use units of centimeters for the diameter, D .

It is well known (Dutton, 1986) that the attenuation per unit length, α_i in decibels per kilometer, at frequency ν_i , can be expressed as

$$\alpha_i = \alpha(\nu_i) = 4.343 \times 10^3 \int_0^{D_{\max}} Q(D, \nu_i) n(D) dD, \quad (2)$$

where D_{\max} is the maximum drop diameter occurring in a given volume of air, and $Q(D, \nu_i)$ is the attenuation cross section in square meters of a spherical raindrop as evaluated from Mie theory (Ishimaru, 1978). We, of course, make the assumption that electromagnetic attenuation theory for spherical droplets used in the right-hand side of (2) can be equated to the observed attenuations, α_i . This is an equation of some invalidity, since a spherical drop is highly idealized, and is most likely the cause of some degree of unrealism in the results obtained from any method that uses such an equation without knowing the magnitude of the error involved. Other more minor effects, such as multiple scattering, are ignored in the equation process (2) as well.

If we insert (1) into (2) we obtain

$$4.343 \times 10^3 \left[b_1 \int_0^{D_{\max}} D^2 Q(D, \nu_i) dD + b_2 \int_0^{D_{\max}} D Q(D, \nu_i) dD + b_3 \int_0^{D_{\max}} Q(D, \nu_i) dD \right] = \alpha_i \quad (3)$$

Now if we let

$$x_{ij} = 4.343 \times 10^3 \int_0^{D_{\max}} D^{3-j} Q(D, \nu_i) dD, \quad j = 1 \text{ to } 3, \quad (4)$$

we can write (3) in matrix form as

$$\underline{Xb} = \begin{pmatrix} x_{11} & x_{12} & x_{13} \\ x_{21} & x_{22} & x_{23} \\ x_{31} & x_{32} & x_{33} \end{pmatrix} \begin{pmatrix} b_1 \\ b_2 \\ b_3 \end{pmatrix} = \begin{pmatrix} \alpha_1 \\ \alpha_2 \\ \alpha_3 \end{pmatrix} = \underline{\alpha}, \quad (5)$$

which can be solved for the coefficient vector, \underline{b} , as

$$\underline{b} = \underline{X}^{-1} \underline{\alpha}. \quad (6)$$

The values x_{ij} can be obtained either by a numerical integration or a polynomial fit to $Q(D, \nu_i)$, both of which are relatively straightforward since $Q(D, \nu_i)$ is monotonic at $\nu_i = 28.8, 57.6, \text{ or } 96.1$ GHz to a D_{\max} of 0.75 cm--the value chosen as an upper limit. A drop larger than 0.75 cm in

diameter is extremely unlikely in the atmosphere. Some of the implications and complications associated with the use of a D_{\max} of 0.75 cm in connection with actual predictions will be discussed in the next section.

3. APPLICATION OF THE PARABOLIC MODEL

Before examining some actual attenuation data to obtain the \underline{b} coefficients, using (6), let us consider some of the problems associated with the actual implementation of that equation. We have obtained results for the x_{ij} 's in (4) by performing a simple trapezoidal-rule numerical integration of the integrand, which can be expressed exactly for a given D and v_i . Integration to a D_{\max} of 0.75 cm yielded*

$$\underline{X} = \begin{pmatrix} 0.06391 & 0.09971 & 0.1648 \\ 0.06053 & 0.09497 & 0.1594 \\ 0.05705 & 0.08951 & 0.1505 \end{pmatrix}. \quad (7)$$

The matrix in (7) contains rows that do not appear significantly different from one another, which could mean that the matrix is "ill-conditioned". Ill-conditioning of \underline{X} in turn could cause the solution (6) to produce spurious and unmeaningful results for \underline{b} in a computer process. There are a number of tests for ill-conditioning, which, in itself, implies that there is no single, simple yardstick for determining whether or not a matrix like \underline{X} is absolutely ill-conditioned. For example, the "condition" of \underline{X} fails a couple of these tests, but one test which it does pass is one involving a check of the product $\underline{X}\underline{X}^{-1}$. If any element involving a check of this product is different from the corresponding element of the identity matrix by more than .001, then \underline{X} can be assumed to be ill-conditioned. However $\underline{X}\underline{X}^{-1}$ yields the identity matrix to at least 4-decimal place accuracy. This test is probably rather crucial, since an implied $\underline{X}\underline{X}^{-1}$ multiplication is contained in the result (6). For this reason, and because \underline{b} results from (6) appear reasonable, we shall assume those results throughout the remainder of this section.

Of course, one can consider models other than the parabolic one of (1)

*Different integration limits will produce different numerical values in (7), but the order of magnitude remains the same, and results are only slightly changed.

for $n(D)$, but the primary reasons for the choice of (1) is that the number of coefficients, b_1 , is equal to the number of frequencies of observation so that an equation such as (6) can be readily obtained, and further it is a direct, first-three-term expression of a Taylor series. A model of the form

$$n(D) = a_1 e^{-a_2 D^2} \quad (8)$$

like the Marshall-Palmer (MP) distribution (Marshall and Palmer, 1948) has too few coefficients ($a_{1,2}$) to be resolved uniquely from the three frequency data [unless, of course, it is expanded similarly to (1)]. Models with three coefficients, and with assorted powers of D , could be used, but there is no real basis for any such choices, at least any more so than (1). For that matter, the MP distribution has no fundamental physical basis either, which should be apparent from its behavior. It does, however, provide a time-honored yardstick for comparison. Clearly, with more frequencies of measurement, more terms could be added to the power series of (1).

Figures 1 through 4 show four separate analyses of rain attenuation data observed during early 1985 in Gasquet, CA, at the three frequencies of 28.8, 57.6, and 96.1 GHz. We shall concentrate our discussion on Figure 1 since it exemplifies all of the four figures. Figures 1 through 4 are subdivided into two graphs per figure. The smaller graph in the upper right-hand corner (dashed-line curves) shows the variation of the observed rain attenuation per kilometer (specific attenuation) versus frequency, and the specific attenuation, α_ν , in decibels per kilometer, derived from the MP distribution as

$$\alpha(\nu) = a(\nu) R^{b(\nu)}. \quad (9)$$

In (9), R is rain rate in millimeters per hour, and $a(\nu)$ and $b(\nu)$ are coefficients dependent upon frequency, ν , that can be obtained from tables in Olsen et al. (1978). A dashed line has been used to join the three actually observed specific attenuations in Figures 1 through 4.

In the lower left-hand corner of Figures 1 through 4 are plotted the resultant drop-size distribution (the solid-line curve) obtained via (6). For comparison the MP drop-size distribution,

$$n(D) = 80,000 \exp(-41R^{-0.21} D), \quad (10)$$

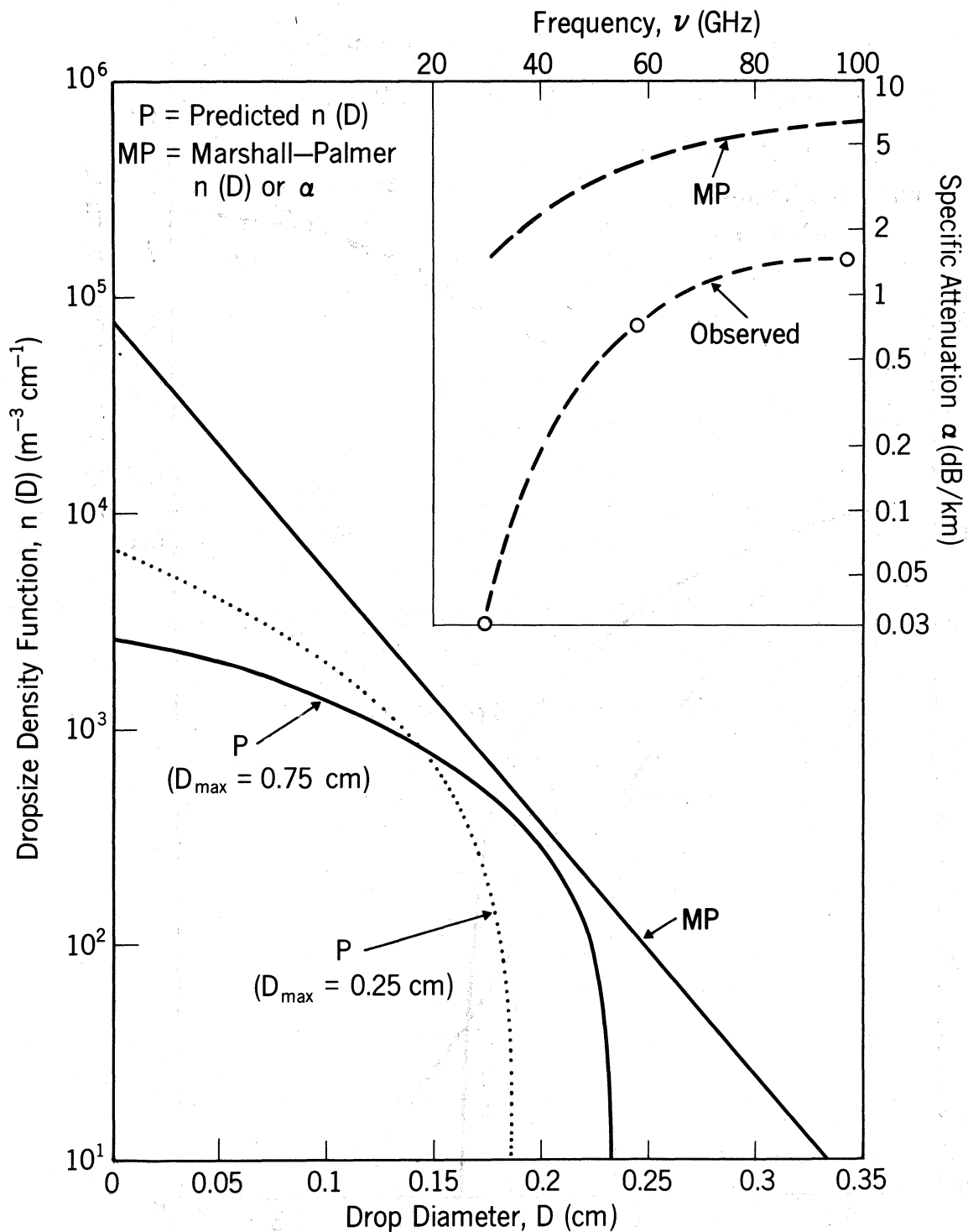


Figure 1. Plots of the drop-size density function (lower left-hand plot) obtained from $n(D) = b_1 D^2 + b_2 D + b_3$ and the Marshall and Palmer (1948) model, and of the specific attenuation versus frequency (upper right hand plot) at Gasquet, CA, February 6, 1985, 2127 hours local time, for a rain rate, $R = 7.34 \text{ mm/h}$.

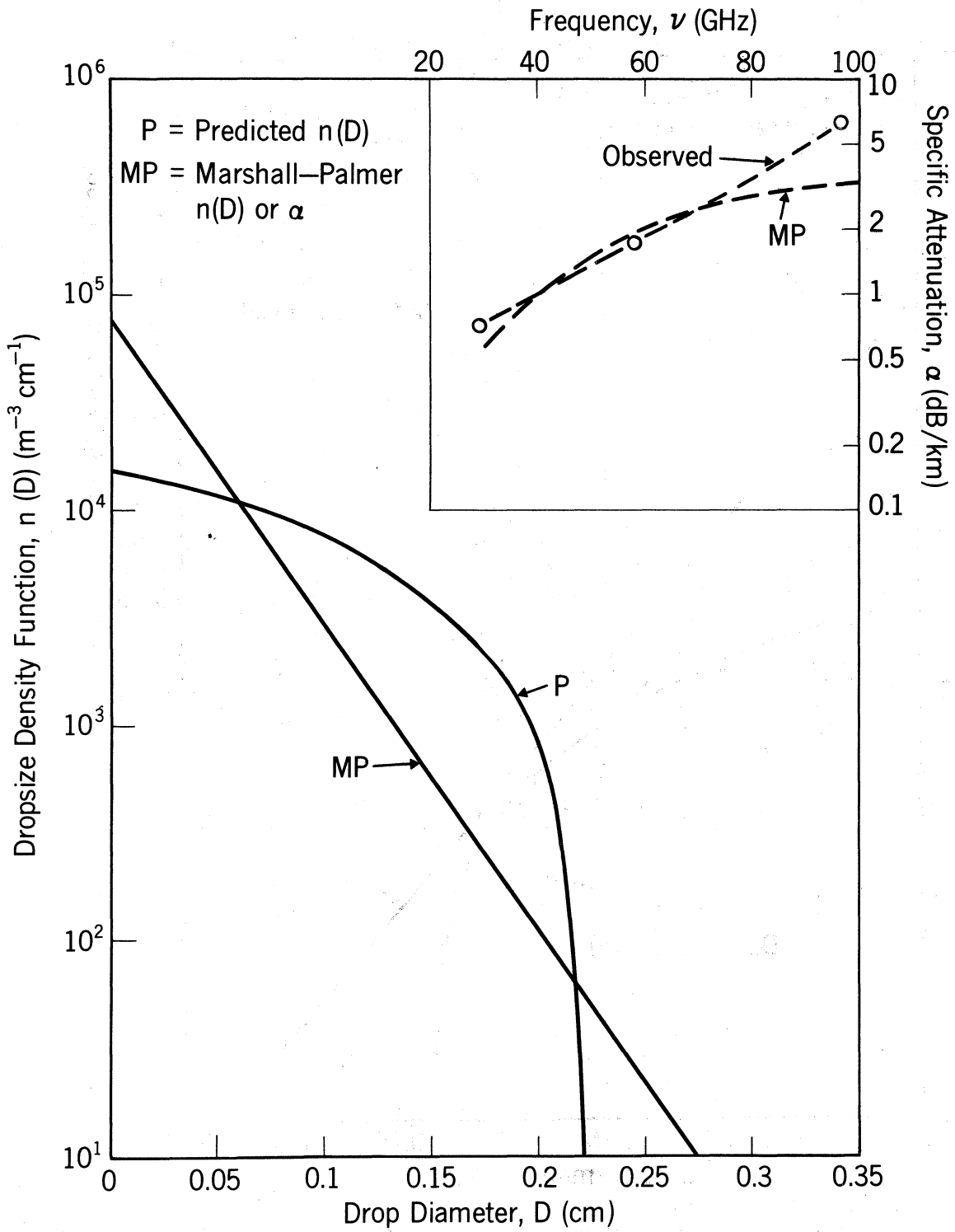


Figure 2. Same as Figure 1 at Gasquet, CA, but for March 20, 1985, 1314 hours local time, for a rain rate $R = 2.96$ mm/h.

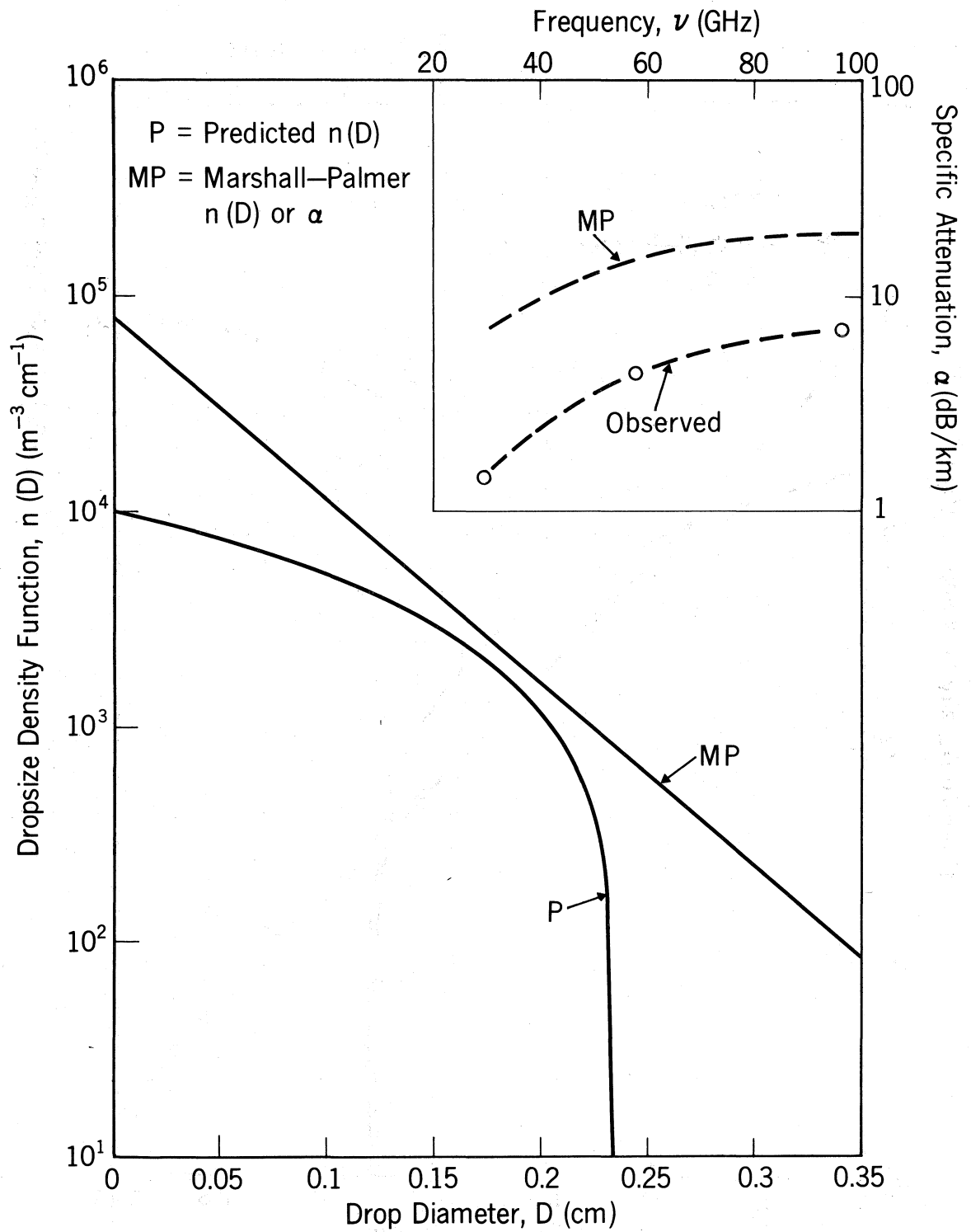


Figure 3. Same as Figure 1 at Gasquet, CA, but for March 23, 1985, 1828 hours local time, for a rain rate $R = 33.26$ mm/h.

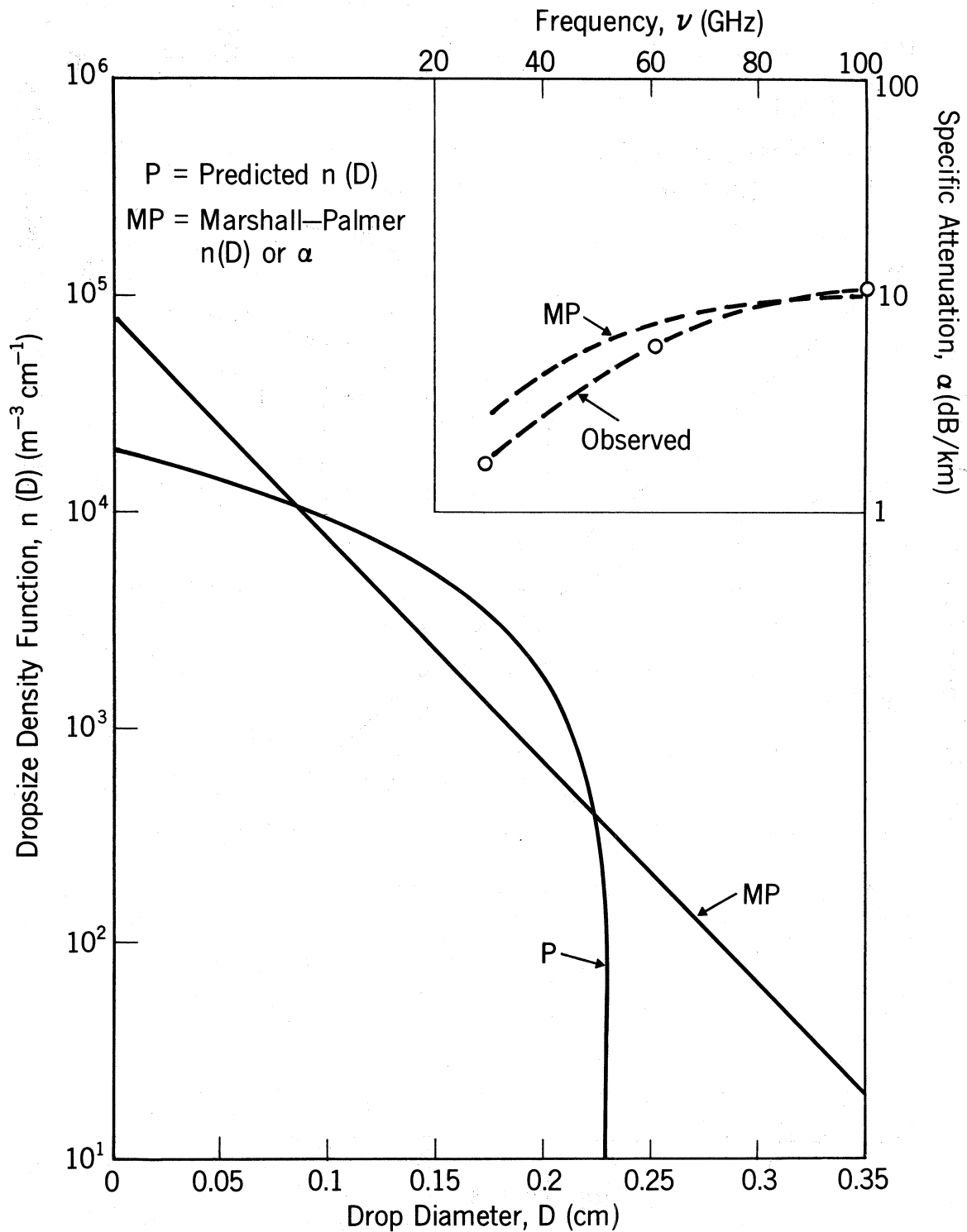


Figure 4. Same as Figure 1 at Gasquet, CA, but representing the 0.1% ($R = 27.2$ mm/h) expectancies of specific attenuation and rainrate.

is shown as the solid, straight line of Figures 1 through 4, where D is in centimeters and $n(D)$ is the number of raindrops per centimeter of diameter spectrum per cubic meter of air ($\text{cm}^{-1}\text{m}^{-3}$).

We shall concentrate our discussion on Figure 1, since it exemplifies all four of the figures. In Figure 1, one notes a third, dashed curve plotted in the lower left-hand graph. Before discussing this curve, we need to explain that while the solid curve in Figures 1 through 4 appears to be a reasonable distribution, there is a slight "hitch" that does not appear in the figures. Remember that (1) is a parabola, and, as such, can have two zero values on the D axis--which, in the cases presented, it does have. In the case of Figure 1, for example, these zero points are at $D = 0.234$ cm, and at $D = 0.664$ cm.

Recalling that the integration (2) extended to $D_{\text{max}} = 0.75$ cm, there is

- 1) a range of position $n(D)$ between $D = 0$ and 0.234 cm,

which is shown on Figure 1.

but, in addition,

- 2) there is a range of negative $n(D)$ between $D = 0.234$ cm and 0.664 cm,

and

- 3) another range of positive $n(D)$ between $D = 0.664$ cm and 0.75 cm,

that contribute to the integral in (2). Items 2) and 3) are clearly not likely physically. Certainly negative drops do not occur, and positive drops above about 0.6 cm are not very likely in the atmosphere. Therefore, in the case of Figure 1, we decided to try to find a value of D_{max} where items 2) and 3) above do not happen, and to check the appearance of the resultant $n(D)$ in that case.

Such a case was nearly obtained by setting $D_{\text{max}} = 0.25$ cm in the upper limit of the integral in (2) for Figure 1. In this situation, zero points are obtained at

$$D = 0.187 \text{ cm,}$$

and at

$$D = 0.283 \text{ cm.}$$

This means that only a small amount of drops in the condition analogous to 2) above resulted, and no drops in the condition analogous to 3) above resulted. Thus the drop-size density function given by the dotted line curve in the lower left-hand graph of Figure 1 is almost representative of the appropriate $n(D)$ to equate the left- and right-hand sides of (2) for the three frequencies of $\nu_1 = 28.8$ GHz, $\nu_2 = 57.6$ GHz, and $\nu_3 = 96.1$ GHz. Note that

the $D_{\max} = 0.25$ cm (dotted) curve of Figure 1 is skewed somewhat toward more small raindrops and fewer larger raindrops per cubic meter, but for the most part the $D_{\max} = 0.25$ cm curve retains the same general appearance as the $D_{\max} = 0.75$ cm (solid) curve in the bottom left-hand graph in Figure 1. Certainly those two curves are much closer in appearance to one another than they are to the MP $n(D)$ curve. As an added qualification, the rain water content, M , of a cubic meter of air was determined for each of the three $n(D)$'s displayed in Figure 1. For the $D_{\max} = 0.25$ cm curve we obtained $M = 0.120 \text{ g/m}^3$, for the $D_{\max} = 0.75$ cm curve we obtained $M = 0.165 \text{ g/m}^3$, but for the MP line we obtained $M = 0.475 \text{ g/m}^3$.

Clearly, the $D_{\max} = 0.75$ cm solution to (6) cannot be established as the ultimate representation of $n(D)$, but in all cases examined, it appears to be a superior representation than the corresponding MP distribution, which, given no other information than is presently available, is probably the only other estimate of $n(D)$ possible. Other choices of D_{\max} are probably better than $D_{\max} = 0.75$ cm, but in lieu of an arduous process of seeking them out, we have chosen to present the $D_{\max} = 0.75$ cm $n(D)$ curves in Figures 1 through 4 as better first approximations of reality than the MP results.

Figure 1 then shows the Gasquet, CA, results for February 6, 1985, at 2127 local time (LT); Figure 2 shows Gasquet results for March 20, 1985, at 1314 LT; and Figure 3 shows Gasquet results for March 23, 1985 at 1828 LT. These are three samples of 1-min averaged rain attenuation results. Figure 4 shows results for the rain rate and attenuations expected 0.1 percent (corresponding to a rain rate $R = 27.2 \text{ mm/h}$) of the time at Gasquet, determined for the total rainy-time sample.

4. CLIMATIC CHARACTERIZATION OF ATTENUATION DISTRIBUTIONS

A technique designed to yield information about the annual distribution of specific rain attenuation (attenuation per kilometer of path length) and its variability at millimeter-wave frequencies was presented in Dutton (1986). This technique gleaned the information from a sample of the daily distributions of 1-min rain attenuation averages made during January and February 1985, at Gasquet, CA. There were nine daily distributions in this sample, to which a quadratic regression procedure was applied, resulting in an estimated mean distribution and a predicted upper bound on the distributions. Two upper bounds were used. First, the standard regression-

prediction upper bound (Crow et al., 1960, p. 163) at the 99.95 percent prediction level was presented. Second, an empirically derived upper bound that is unchanged from the first bound at higher exceedance percentiles, but is a factor of three farther from the estimated mean distribution than the first bound at lower percentiles, was included. For this particular situation, the second bound encompassed all the sample distributions, and even three later additional daily rain attenuation distributions taken in March 1985, at Gasquet. Not unexpectedly, the first bound did not encompass all these distributions, often missing the critical rare-event region. Whether the second bound is superior to the first bound is, however, still not immediately clear. This is primarily because of the fact that although the second bound does apparently envelope all the sample distributions, it may not be economically feasible to incorporate such high attenuation values into link-design fade margins. In the analyses that follow, the results do little to identify which bound is superior, so that the choice of an appropriate upper bound between the two presented is still left at the option of a given user.

Enough rain attenuation data have now been acquired to develop a macro-scale (large scale) climatic characterization of predicted rain attenuation distributions at 28.8, 57.6, and 96.1 GHz for the United States. This characterization will subdivide the United States (excluding Alaska and Hawaii) into three rain and/or millimeter-wave rain attenuation climates, with a representative location where millimeter-wave rain attenuation data were taken in each climatic type (zone).

These three climatic types can be described as:

- 1) Maritime temperate, represented by Gasquet, CA,
- 2) dry-continental temperate, represented by Boulder, CO,

and

- 3) humid-continental temperate, represented by Huntsville, AL.

This is, as a matter of necessity, a somewhat different climatological classification than the more standard ones (e.g., Koppen, 1918), because of the small number of data-acquisition locations. Figure 5 shows a map of the United States with zones roughly corresponding to the three climatic classifications sketched thereon. In the next section, then, the analysis of data and the correspondingly derived annual rain attenuation distribution and its bounds for the first two of the three climatic-representative stations at

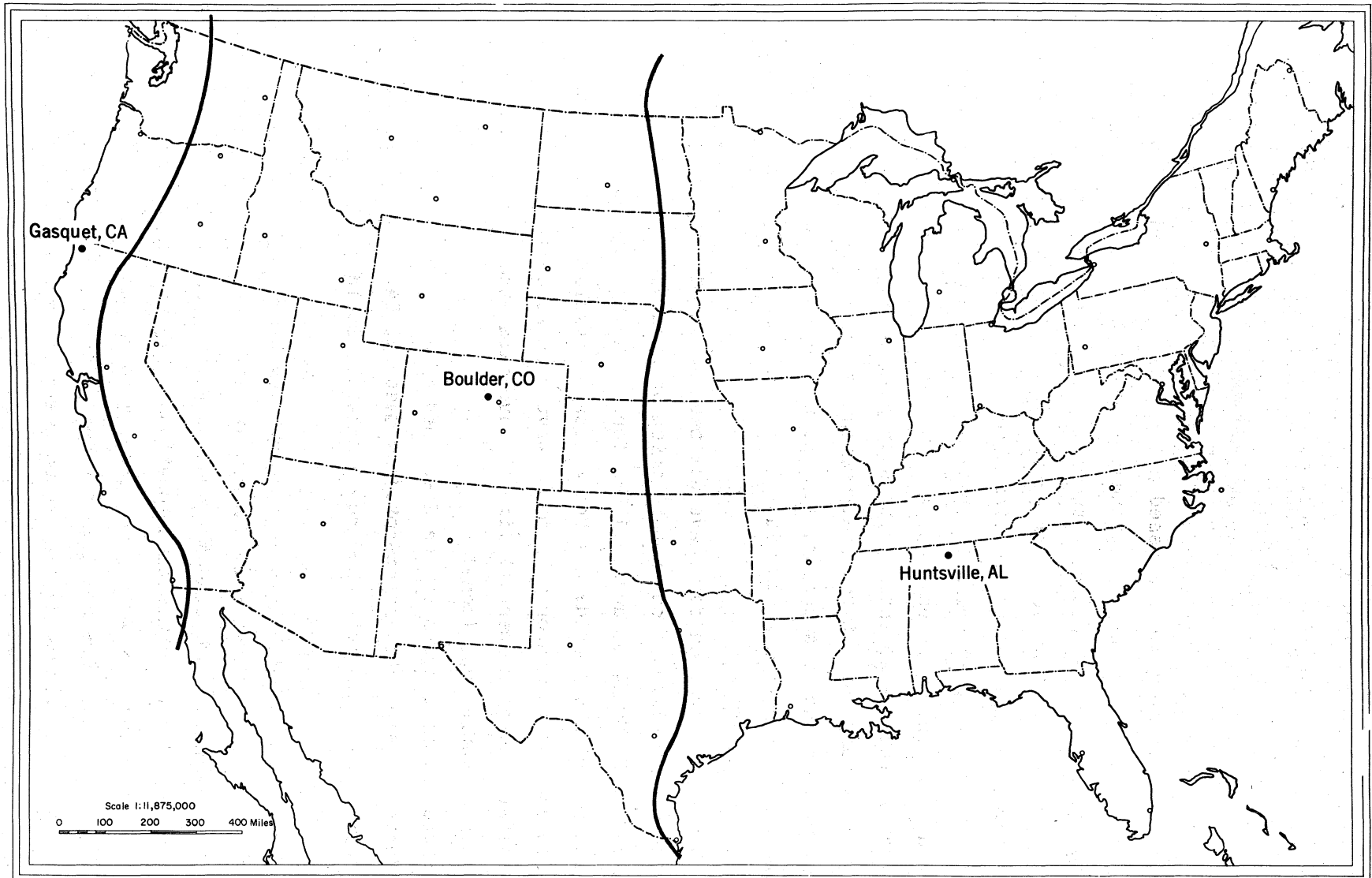


Figure 5. A three-rainfall zonal division of CONUS for millimeter-wave rain attenuation prediction purposes. Small circles indicate some major urban weather-observing locations in CONUS.

28.8, 57.6, and 96.1 GHz will be discussed. Clearly, a mere three climatic classifications will not be adequate for representation of every location in the zones of Figure 5, but hopefully will provide a step in the right direction.

5. ANALYSIS OF RECENT RAIN ATTENUATION DISTRIBUTIONS

As mentioned in Section 3, only three March 1985, daily specific rain attenuations were compared with the regression results for Gasquet, CA, in Dutton (1986). These were obtained on the days of March 20, 21, and 22, 1985. Before data acquisition was completed at Gasquet, CA, however, daily distributions for March 23, 24, 25, and 26, 1985, were also available. When these distributions were compared with the 9-day distribution "standard sample" for Gasquet, presented in Dutton (1986), results were not nearly so encouraging, since some of the data for the 23rd and 24th of March exceeded even the second bound at 28.8 GHz. As a consequence it was decided to use all the daily distributions (16 total) as a single data base from which to derive the mean and the two upper bound distributions for the three frequencies of 28.8, 57.6, and 96.1 GHz at Gasquet. This is discussed in the next subsection.

5.1 Distributional Analysis at Gasquet, California

Figures 6 through 11 show the 16 daily specific rain attenuation distributions, in decibels per kilometer, for the January 27 through March 26, 1985, observation period at Gasquet, CA. As indicated in Dutton (1986), Gasquet was chosen because of its considerable annual rainfall (2431 mm average) occurring principally during the winter, its proximity to electrical power and rainfall measurement facilities (Gasquet Ranger Station), and adequate open terrain for the establishment of a nearly 1 km (1.003 km) link. The distributions obtained by unweighted quadratic regression (Dougherty and Dutton, 1984) will be taken as representative of the average annual specific rain attenuation distribution and its two upper bounds for a maritime temperate climate, as discussed in Section 4.

Figure 6 shows the 28.8 GHz set of 16 daily distributions, along with the regressed mean distribution and its 99.95 percent upper confidence limit. A couple of distributions--those for the 23rd and 24th of March 1985--exceed the 99.95 percent bound by a considerable margin, suggesting that the 99.95

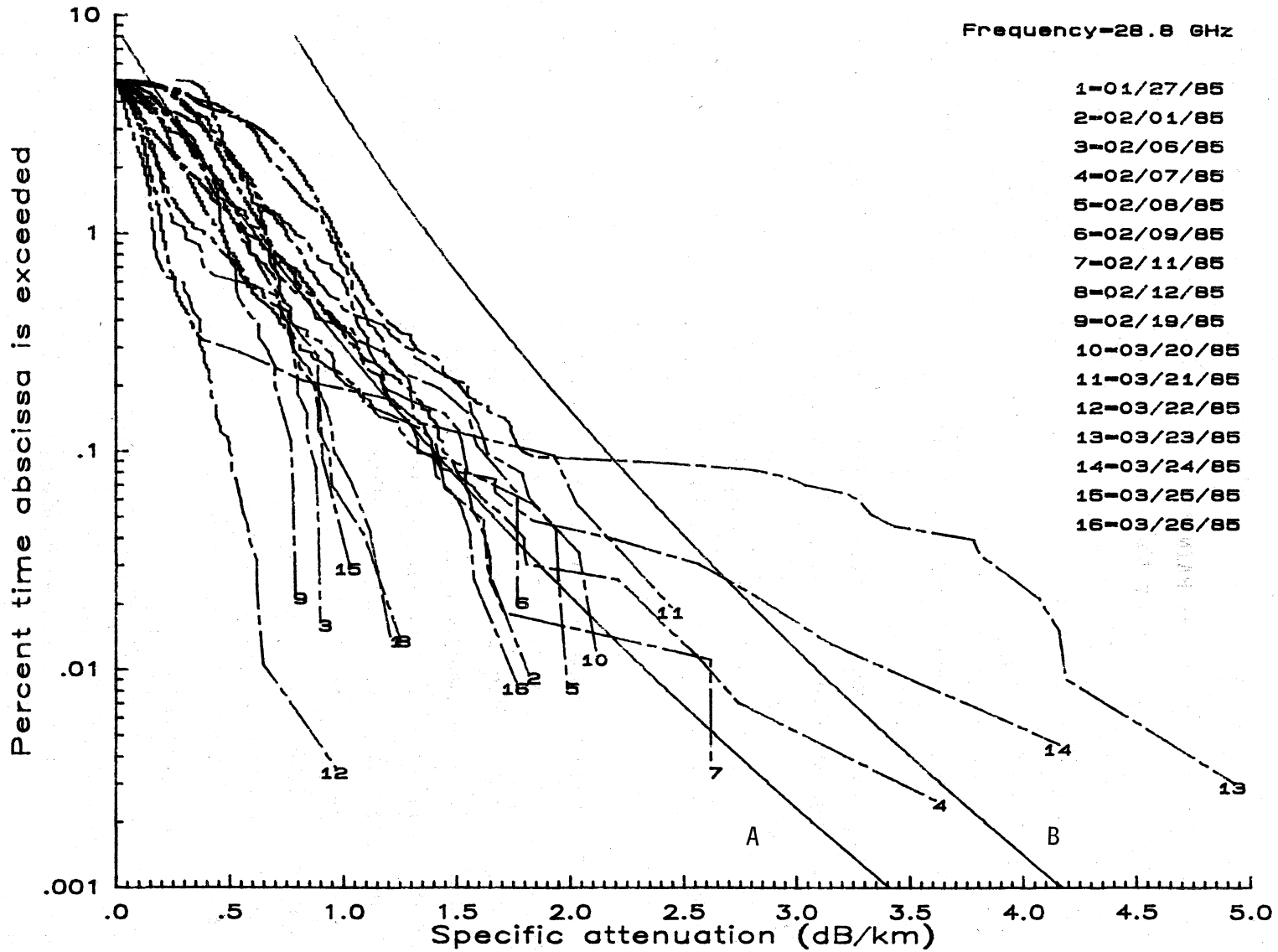


Figure 6. Quadratic regression best-fit (curve A) and 99.95% prediction bound (curve B) to the January 27 to March 26, 1985, sample of daily specific rain attenuation distributions for Gasquet, CA, at 28.8 GHz.

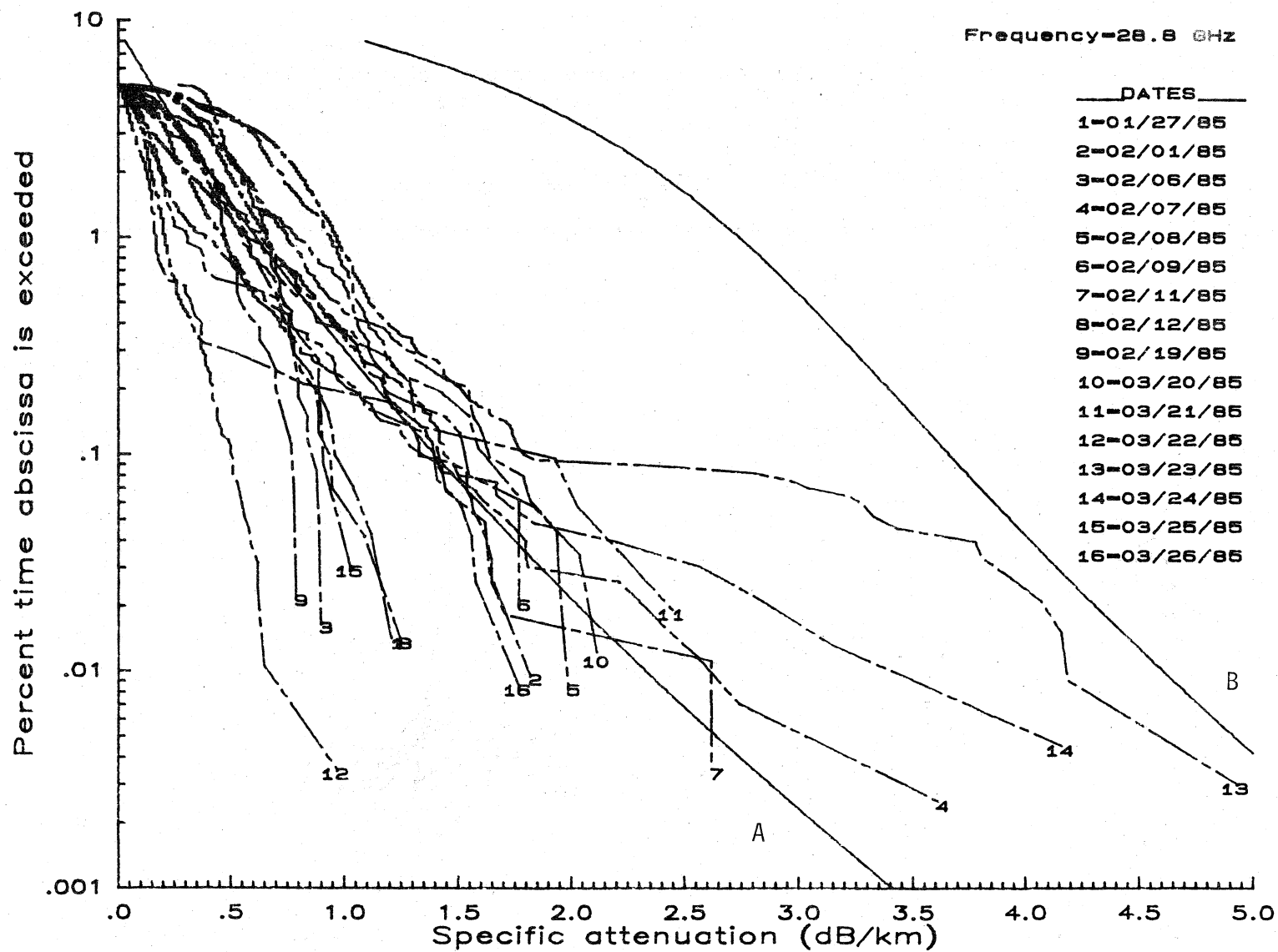


Figure 7. Quadratic regression best-fit (curve A) and an empirically derived upper bound distribution (curve B) for the January 27 to March 26, 1985, sample of daily specific rain attenuation distributions for Gasquet, CA, at 28.8 GHz.

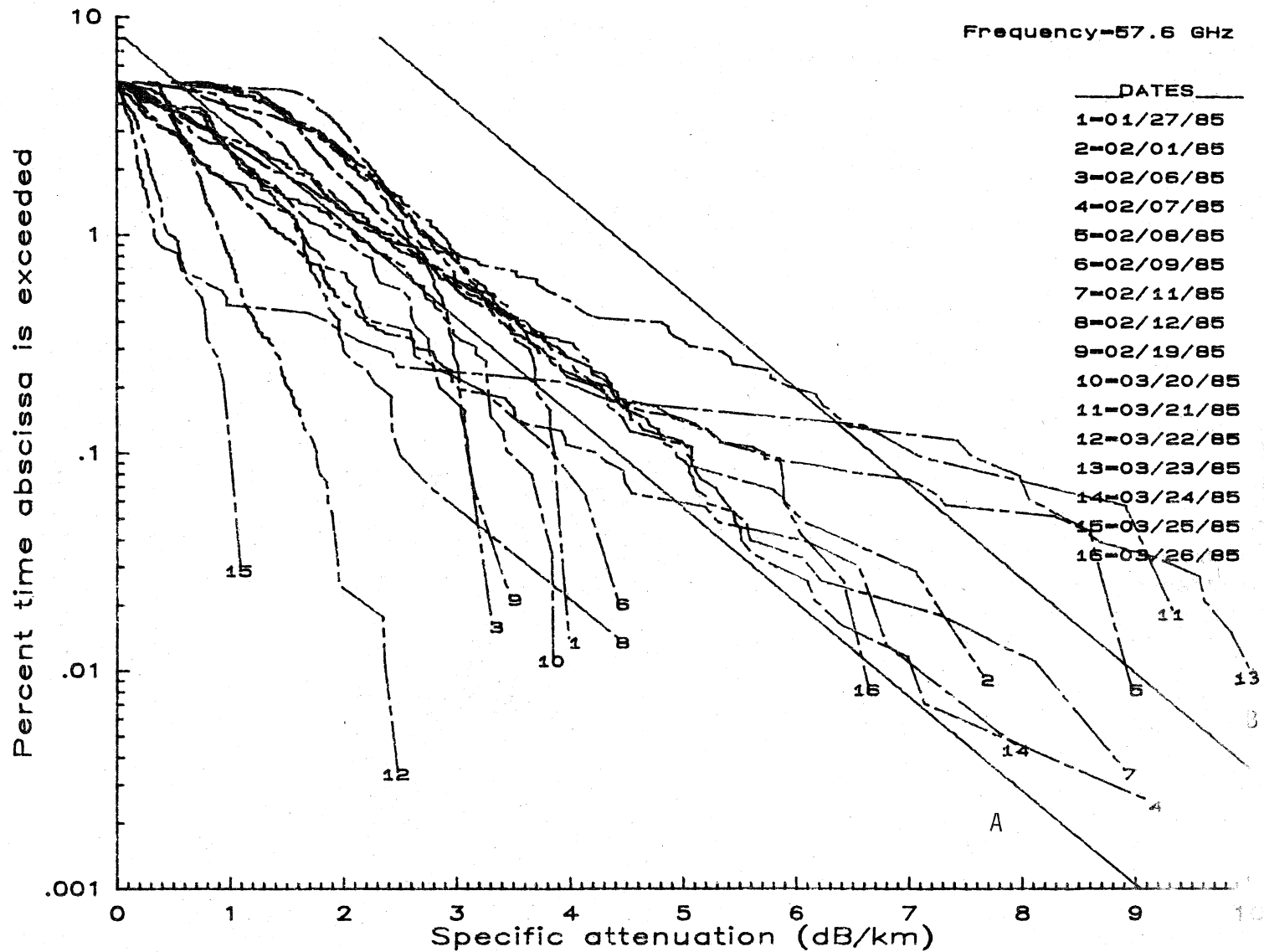


Figure 8. Quadratic regression best-fit (curve A) and 99.95% prediction bound (curve B) to the January 27 to March 26, 1985, sample of daily specific rain attenuation distributions for Gasquet, CA, at 57.6 GHz.

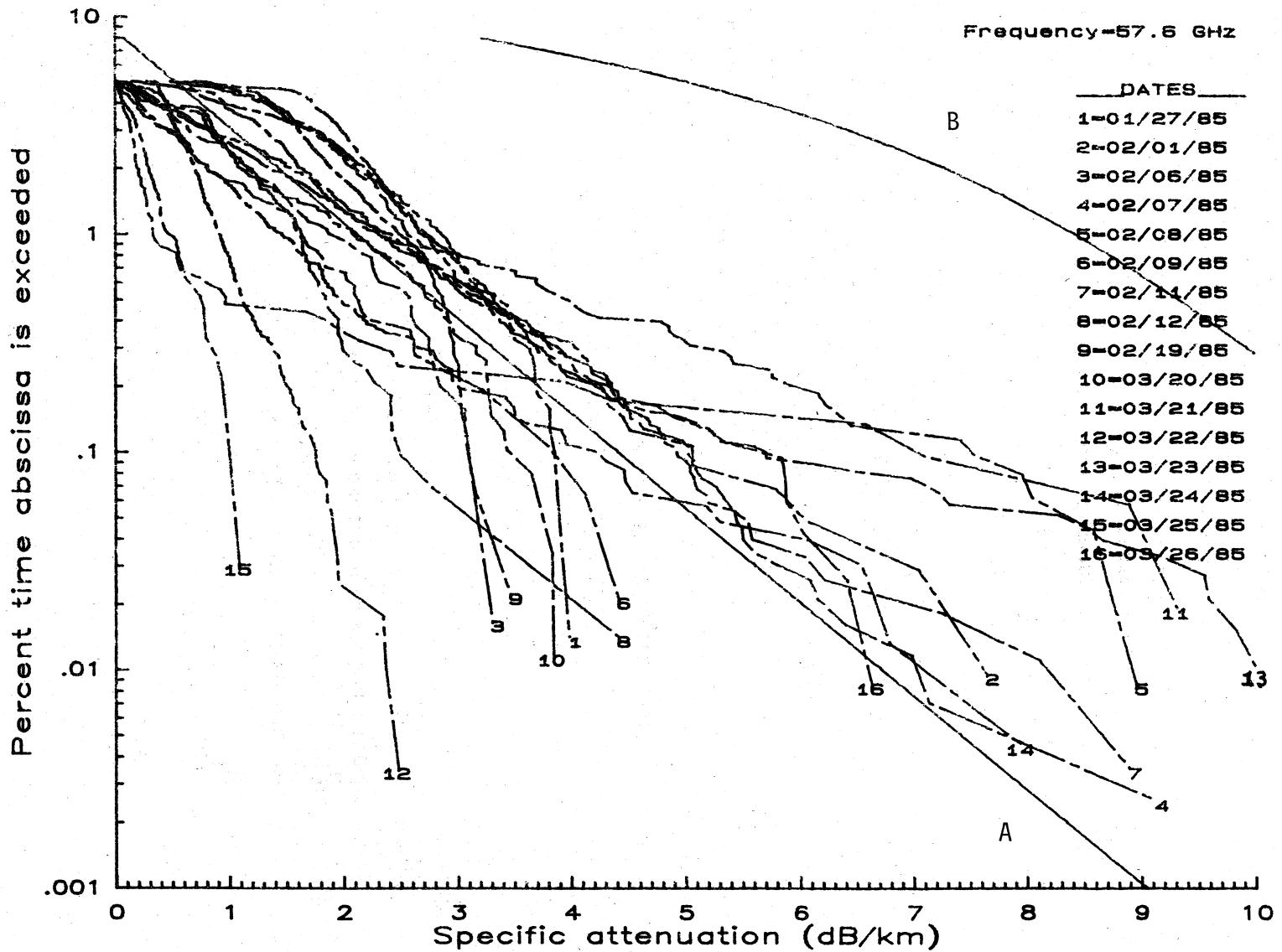


Figure 9. Quadratic regression best-fit (curve A) and an empirically derived upper bound distribution (curve B) for the January 27 to March 26, 1985, sample of daily specific rain attenuation distributions for Gasquet, CA at 57.6 GHz.

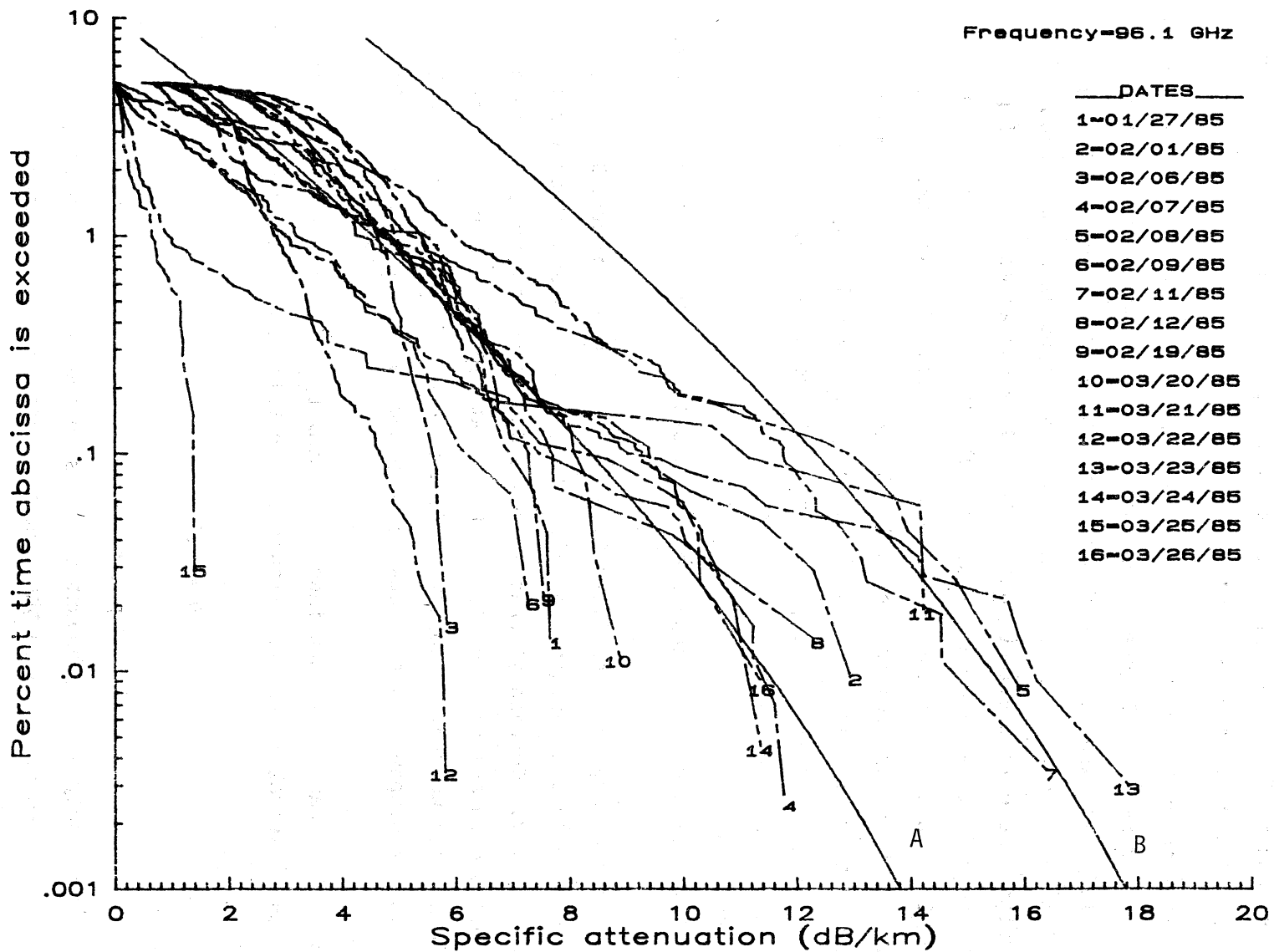


Figure 10. Quadratic regression best-fit (curve A) and 99.95% prediction bound (curve B) to the January 27 to March 26, 1985, sample of daily specific rain attenuation distributions for Gasquet, CA, at 96.1 GHz.

percent bound is not a satisfactory delimiter for the 28.8-GHz situation. Figure 7 is identical to Figure 6, except that the 28.8-GHz empirical upper bound (EUB) is presented. In this situation the EUB appears to be a quite satisfactory delimiter of the data presented, exceeding the worst daily distribution shown by only a slight margin.

Figure 8 shows the 57.6 GHz set of 16 daily distributions, together with the regressed mean distribution and its 99.95 percent upper confidence limit. Here, three of the daily distributions--those of February 8, March 21, and March 23, 1985--exceed the 99.95 percent upper bound by a sufficient enough margin to conclude that the 99.95 percent bound is probably not a satisfactory delimiter for the 57.6-GHz attenuation distribution at Gasquet. Figure 9 is identical to Figure 8 except that the 57.6 GHz EUB is substituted for the 99.95 percent prediction upper bound. Here, however, the EUB seems much too large. While the EUB does encompass all the 57.6 GHz daily distributions for the Gasquet sample, it is nevertheless not the most conservative bound, and as a result is likely not economically attractive.

Figure 10 shows the 96.1 GHz set of 16 daily distributions, with their regressed mean distribution and the 99.95 percent upper prediction confidence limit. At this lone frequency, the 99.95 percent bound does a fairly reasonable job of bounding the daily distributions, even though at places the February 8, March 21, and March 23, 1985, distributions do slightly exceed the bound. Figure 11 is identical to Figure 10 except that it shows the EUB for 96.1 GHz instead of the 99.95 percent bound. As is the case at 57.6 GHz the 96.1 GHz EUB appears to be far too excessive a bound on the daily distributions, regardless of the fact that it does encompass all 16 daily distributions. So, as noted earlier, this extended analysis of the data for Gasquet, CA, beyond that presented in Dutton (1986), has done little to identify a clear choice between the 99.95 percent upper prediction confidence limit and the EUB as to which is the best for design purposes. Hence, that choice, or some other choice is still left to the volition of the system designer.

5.2 Distributional Analysis at Boulder, Colorado

Figures 12 through 17 show 13 daily 1-min-average specific rain attenuation distributions in decibels per kilometer for the period May 19 through July 24, 1985, at Boulder, CO. In Dutton (1986), distributional

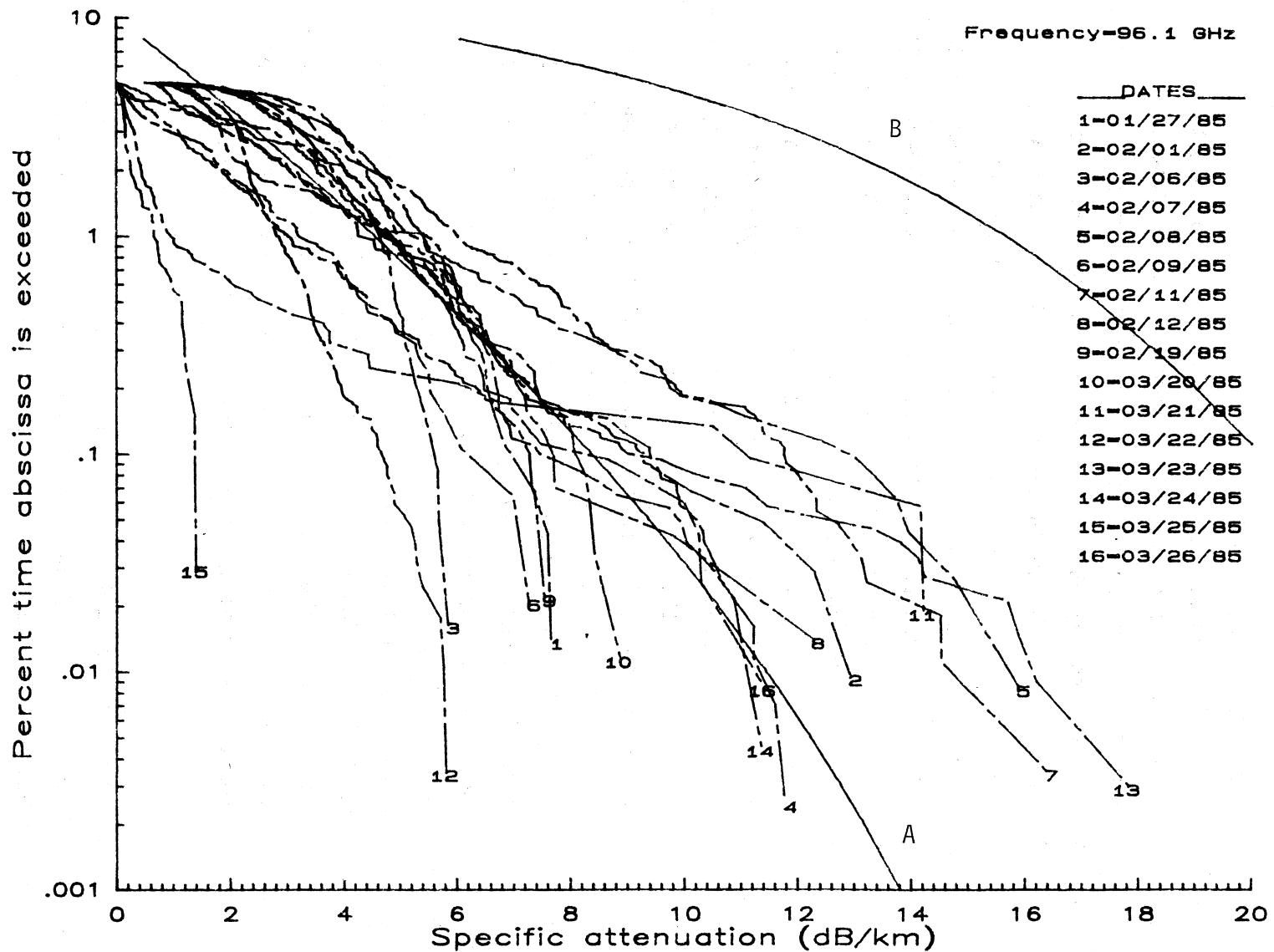


Figure 11. Quadratic regression best-fit (curve A) and empirically derived upper bound distribution (curve B) for the January 27 to March 26, 1985, sample of daily specific rain attenuation distributions for Gasquet, CA, at 96.1 GHz.

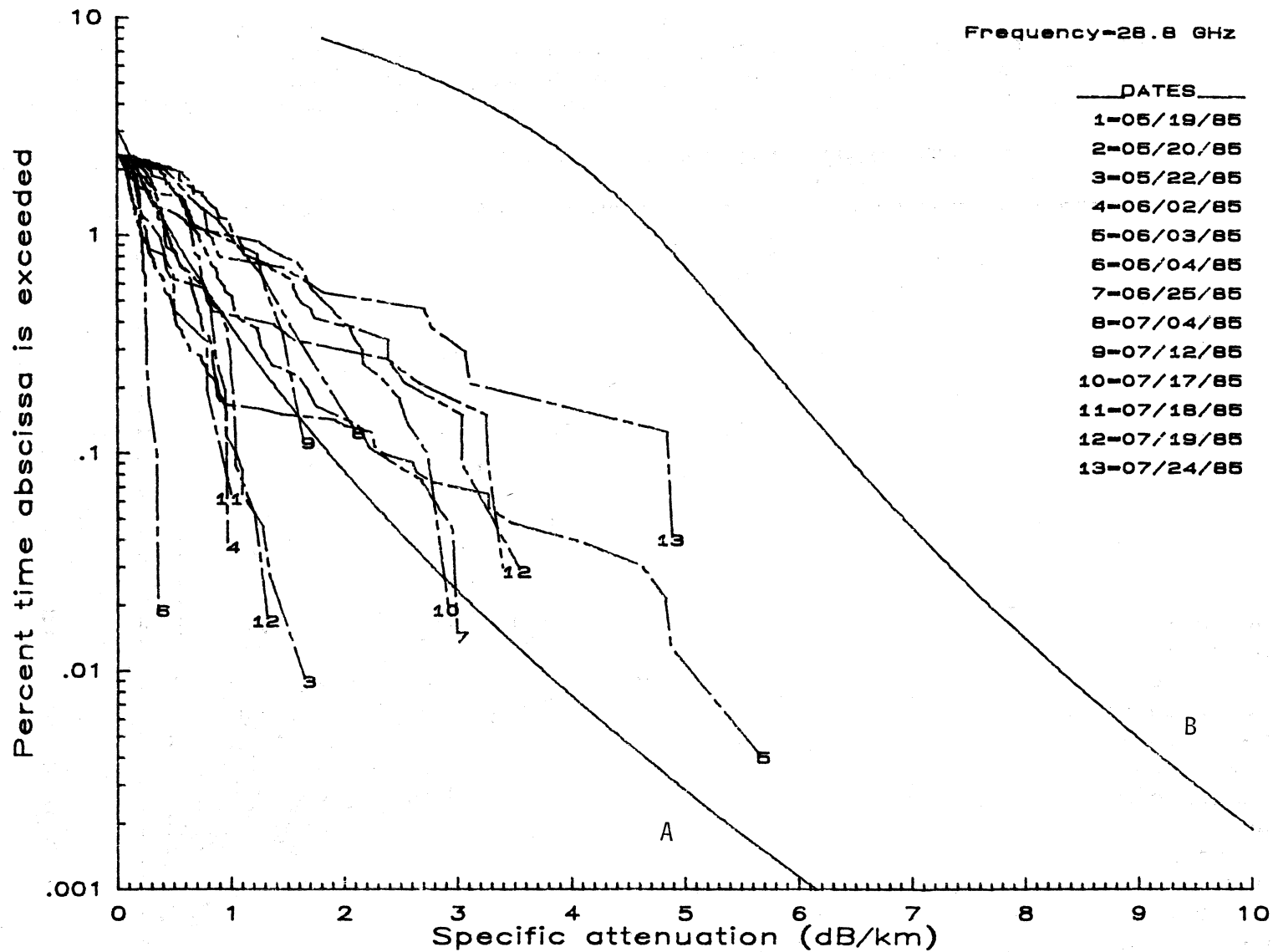


Figure 13. Quadratic regression best-fit (curve A) and an empirically derived upper bound distribution (curve B) for the May 19 to July 24, 1985, sample of daily specific rain attenuation distributions for Boulder, CO, at 28.8 GHz.

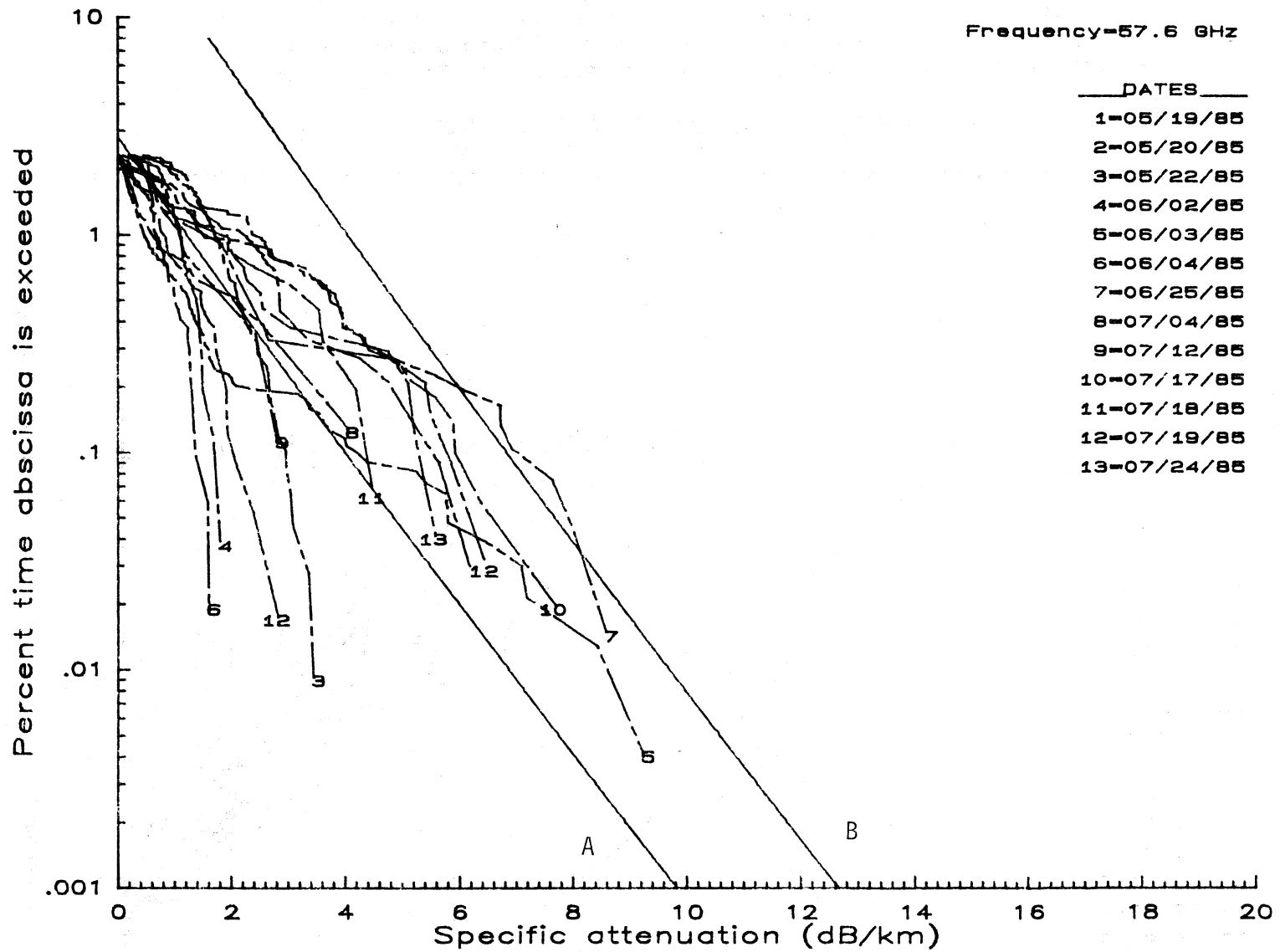


Figure 14. Quadratic regression best-fit (curve A) and 99.95% prediction bound (curve B) to the May 19 to July 24, 1985, sample of daily specific rain attenuation distributions for Boulder, CO at 57.6 GHz.

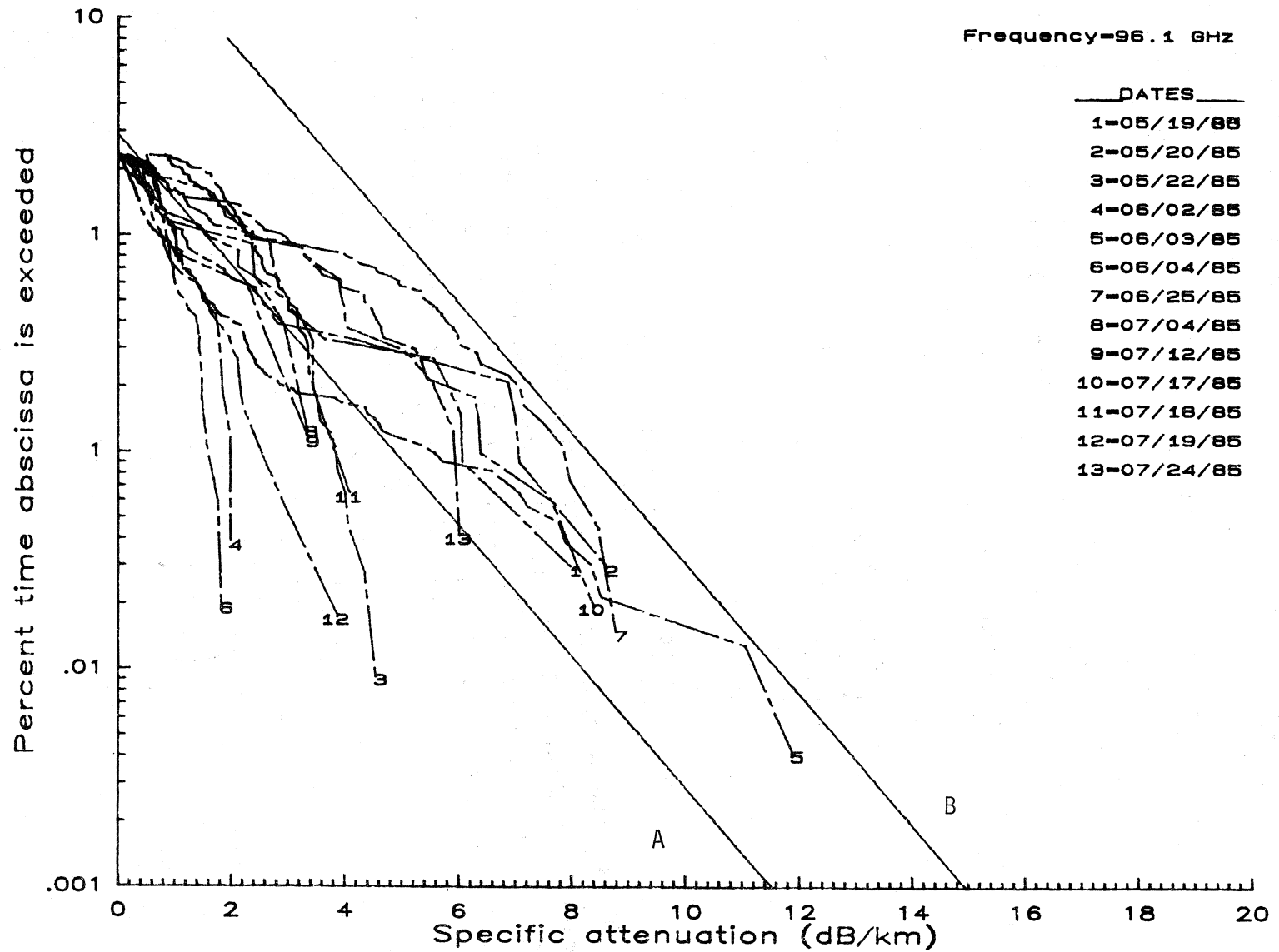


Figure 16. Quadratic regression best-fit (curve A) and 99.95% prediction bound (curve B) to the May 19 to July 24, 1985, sample of daily specific rain attenuation distributions for Boulder, CO, at 96.1 GHz.

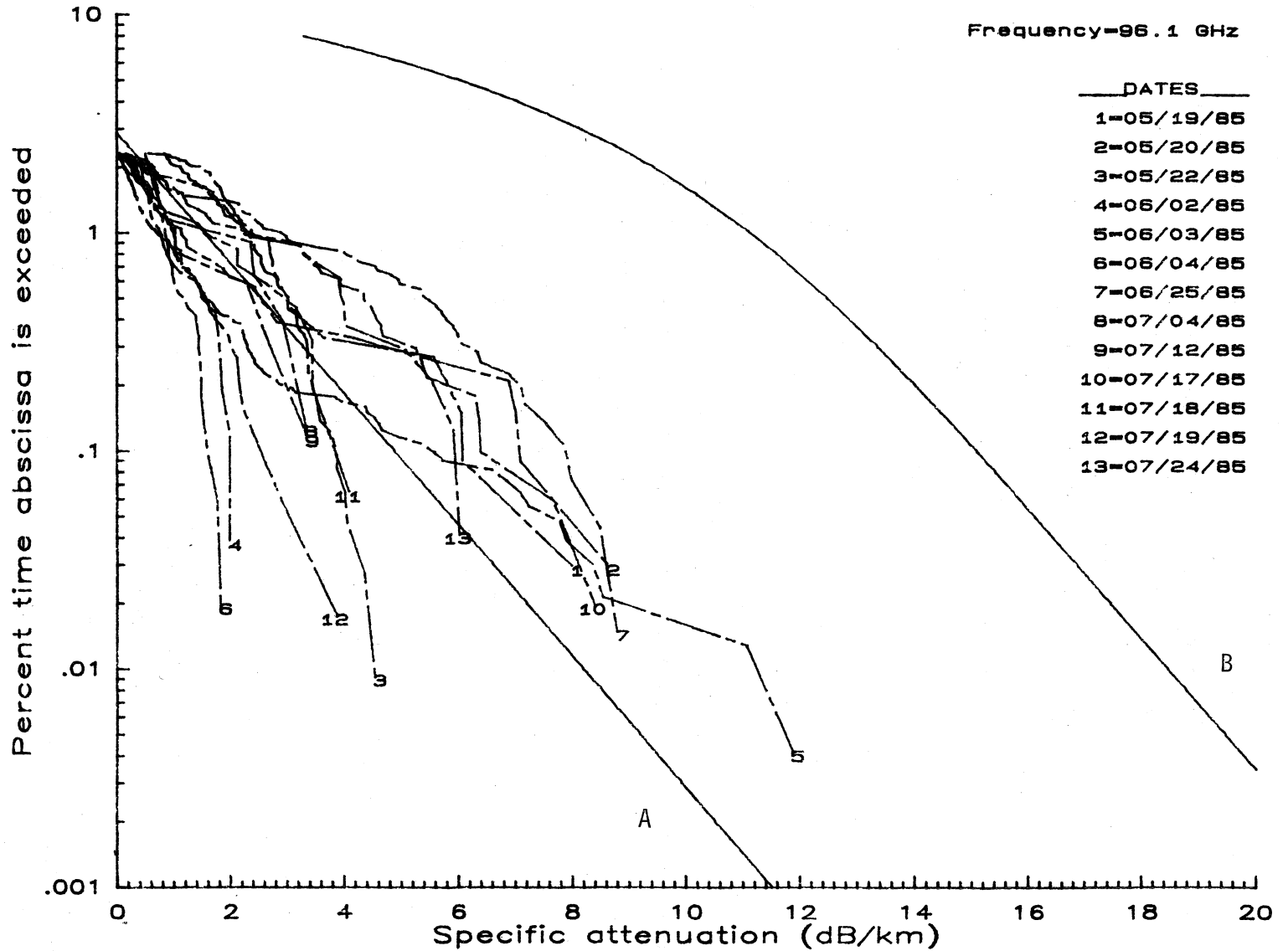


Figure 17. Quadratic regression best-fit (curve A) and an empirically derived upper bound distribution (curve B) for the May 19 to July 24, 1985, sample of daily specific rain attenuation distributions for Boulder, CO, at 96.1 GHz.

representations for Boulder, CO, were given for data taken during the summer of 1984, but these data were generally intermittent and sparse. Hence, it was decided to repeat the experiment in the summer of 1985. The 1985 Boulder data, then, were of a more extensive and useful nature, primarily because of the experience now acquired in the acquisition of such data. The 1984 Boulder rain data were the first taken in the millimeter-wave experiment.

Boulder, of course, was chosen because it is the location of ITS and the many facilities of the U.S. Department of Commerce, Boulder Laboratories were available. The 1985 Boulder specific rain attenuation observations were made on a 300-m link directly south of the Department of Commerce, Boulder Laboratories, main building, but unlike the 1984 data (Dutton, 1986), specific attenuations were directly recorded. The distributions obtained by the quadratic regression procedure applied to the 13 daily distributions at Boulder during 1985 will be taken as representative of the average annual specific rain attenuation distribution and its two upper bounds for a dry-continental temperate climate (see Section 4.).

Figure 12 shows the 28.8-GHz set of 13 Boulder daily distributions of specific attenuation, together with the regressed mean distribution and its 99.95 percent upper confidence limit. The 99.95 percent limit nearly encompasses all the 13 daily distributions except the one for July 24, 1985. Slight portions of the distributions for May 19 and June 3, 1985, also exceed the 99.95 percent limit, but, in general, the 99.95 percent limit appears to be a fairly reasonable upper bound in spite of this. Figure 13 repeats Figure 12 at 28.8 GHz, except the EUB has replaced the 99.95 percent limit bound. In the case of Figure 13, the EUB appears to be much too generous a bound to be meaningful from the point of view of design economics, particularly for the high system-availability requirements. Figure 14 shows the 57.6-GHz set of 13 Boulder 1985 daily distributions, together with the regressed mean distribution and its 99.95 percent upper confidence limit. In this case, the 99.95 percent limit does an even better job than the corresponding 28.8-GHz delimiter of Figure 12. Only the daily specific attenuation distribution for June 25, 1985, lies slightly above the 99.95 percent limit, while the remaining 12 distributions are encompassed by it. Figure 15 is again identical to Figure 14, except that the EUB replaces the 99.95 percent upper limit bound in that figure. As was the case at 28.8 GHz, the 57.6-GHz EUB of Figure 15 appears an excessive delimiter, with too much attenuation tolerance

at all percentile levels for reasonably economical fade margin design.

Figure 16 shows the 96.1-GHz set of 13 Boulder 1985 daily distributions, the regressed mean distribution, and its 99.95 percent prediction upper confidence limit. The 99.95 percent bound encloses all the data distributions in this sample situation, even though in the population situation (Dutton, 1986) it should not do so. Hence, the 99.95 percent bound for the 96.1-GHz data is an apparently entirely adequate upper bound. Figure 17 is identical to Figure 16 except that the EUB is shown instead of the 99.95 percent bound. Once again, the 96.1-GHz EUB contains a good deal of fade margin protection overkill, should it be used as a design criterion for millimeter-wave communications links.

Unlike the analysis conclusions for Gasquet, CA, presented in Section 5.1, then, we can see a trend for the 1985 Boulder distributional analysis, at least for the sample treated herein. The 99.95 percent prediction upper confidence limit provides an adequate delimiter for fade-margin design purposes, whereas the EUB seems excessive for the three frequencies at 28.8, 57.6, and 96.1 GHz.

6. CONCLUSION

Another method has been developed to obtain the path-averaged raindrop size distribution from specific attenuations observed in the ITS millimeter-wave experiment at the frequencies of 28.8, 57.6 and 96.1 GHz. This method yields a quadratic fit given by (1) to the drop-size distribution. While there are clearly constraining features of such a fitting procedure, which may well tend to produce aberrations to the "actual" drop-size distribution, results appear considerably more plausible than was the case with the earlier method of Dutton and Steele (1984).

Statistical mean and upper bound distributions have been developed from the 1985 ITS millimeter-wave experiment data for a maritime climate, represented by Gasquet, CA; and a dry-continental temperate climate, represented by Boulder, CO. At the writing of this report, insufficient data had been obtained for the humid-continental temperate climate, represented by Huntsville, AL, for adequate analysis to complete the triad of descriptions for the zonal representation in Figure 5 of CONUS rain-attenuation climates. This climatology remains the ultimate goal.

7. ACKNOWLEDGMENTS

The author appreciates the advice and commentary on the modeling provided by the ITS millimeter-wave program project leader, K.C. Allen. Also, the computer programming efforts of D.C. Hyovalti of ITS and L. Nesbitt of the University of Colorado have assisted the author immensely in the production of this report.

8. REFERENCES

- Crow, E.L., F.A. Davis, and M.W. Maxfield (1960), *Statistics Manual* (Dover Publications, Inc., New York, NY), p. 163.
- Dougherty, H.T., and E.J. Dutton (1984), The evaluation of prediction models for microwave attenuation by rainfall, NTIA Report 84-145, February, 40 pp. (NTIS* Order No. PB84-182104).
- Dutton, E.J. (1986), The millimeter-wave behavior of rain attenuation based on recent experimental data, NTIA Report 86-189, January, 44 pp. (NTIS* Order No. PB86-166907).
- Dutton, E.J., and F.K. Steele (1984), Some further aspects of the influence of raindrop-size distributions on millimeter-wave propagation, NTIA Report 84-169, December, 36 pp. (NTIS* Order No. PB85-168334).
- Espeland, R.H., E.J. Violette, and K.C. Allen (1986), Rain attenuation measurements at 28.8, 57.6, and 96.1 GHz on a 1-km path, NTIA Report 86-190, February 44 pp. (NTIS* Order No. PB86-175569).
- Ishimaru, A., (1978), *Wave Propagation and Scattering in Random Media, Volume 1: Single Scattering and Transport Theory* (Academic Press, New York, NY), pp. 27-30.
- Köppen, W. (1918), Klassifikation der Klimate nach Temperatur, Niederschlag, und Jahreslauf, *Pertermanns Mitt. aus Justus Perthes, Geog. Ausf. 64*, pp. 193-248.
- Marshall, J.S., and W. McK. Palmer (1948), The distribution of raindrops with size, *J. Met. 5*, pp. 165-166.
- Olsen, R.L., D.V. Rogers, and D.B. Hodge (1978), The aR^b relation in the calculation of rain attenuation, *IEEE Trans. Ant. Prop. AP-28*, No. 2, pp. 318-329.
- Westwater, E.R., and O.N. Strand (1972), *Inversion Techniques*, Chapter 16 of *Remote Sensing of the Troposphere*, V.E. Derr, Editor, (U.S. Government Printing Office, Washington, D.C. 20402).

* National Technical Information Service (NTIS), 5285 Port Royal Road, Springfield, VA 22161.

BIBLIOGRAPHIC DATA SHEET

1. PUBLICATION NO. NTIA Report 86-201		2. Gov't Accession No.	3. Recipient's Accession No.
4. TITLE AND SUBTITLE Effects of Drop-size Distribution and Climate on Millimeter-wave Propagation Through Rain		5. Publication Date August 1986	6. Performing Organization Code NTIA/ITS.S3
7. AUTHOR(S) E. J. Dutton		9. Project/Task/Work Unit No. 9108108	
8. PERFORMING ORGANIZATION NAME AND ADDRESS U.S. Department of Commerce National Telecommunications & Information Administration Institute for Telecommunication Sciences/S3 325 Broadway Boulder, CO 80303-3328		10. Contract/Grant No.	
11. Sponsoring Organization Name and Address U.S. Department of Commerce National Telecommunications & Information Administration Herbert C. Hoover Building 14th & Constitution Ave., NW, Washington, DC 20230		12. Type of Report and Period Covered	
14. SUPPLEMENTARY NOTES		13.	
15. ABSTRACT (A 200-word or less factual summary of most significant information. If document includes a significant bibliography or literature survey, mention it here.) The distribution of raindrop sizes in a given volume of air remains an unknown aspect of critical importance to the prediction of rain attenuation at millimeter-wave frequencies. Thus, in this report, the search continues for a methodology of predicting drop-size distribution with more apparent success than with earlier procedures developed by this author. The latest method involves prediction of the coefficients of a quadratic fit to the drop-size distribution. Climatology of rain attenuation also is pursued in this report with more data from the Institute for Telecommunication Sciences' (ITS) millimeter-wave experiment undergoing analysis and statistical examination to try to determine bounds on the specific attenuation that could be expected in a maritime climate (Gasquet, CA) and a dry-continental, temperate climate (Boulder, CO). The data analyzed were all taken in 1985 at the three frequencies of 28.8, 57.6, and 96.1 GHz. Observed data were lumped into 1-min average specific rain attenuations for analysis purposes in this report.			
16. Key Words (Alphabetical order, separated by semicolons) attenuation climatology; attenuation distribution; millimeter waves; rain attenuation; raindrop size distribution			
17. AVAILABILITY STATEMENT <input checked="" type="checkbox"/> UNLIMITED. <input type="checkbox"/> FOR OFFICIAL DISTRIBUTION.		18. Security Class. (This report) UNCLASSIFIED	20. Number of pages 38
		19. Security Class. (This page) UNCLASSIFIED	21. Price:

